Needle-tip localization using an optical fibre hydrophone

Jean Martial Mari*[a], Simeon West[b], Paul C. Beard[a], Adrien E. Desjardins[a]

[a]Department of Medical Physics and Bioengineering, University College London, London, United Kingdom; [b]University College Hospital, London, United Kingdom

ABSTRACT

Ultrasound imaging is frequently used for guiding needles during minimally invasive procedures, but accurate identification of the needle tips can be challenging, even for experienced practitioners. In this study, a novel method for tracking needles inside the human body was developed. This method, called ultrasonic device tracking (UDT), involved the detection of ultrasound pulses from the external imaging probe with an optical fibre hydrophone integrated into the needle cannula. Two methods for estimating the needle tip position that were based on the maximum and the centroid of the optical fibre hydrophone signal were tested. The variability of the position estimates is measured at different distances to the electronic focus. The maximum longitudinal variability was less than 80 µm for all distances. The lateral variability remains below 500 µm in a 20 mm region around the focus, but increases up to several mm away from the electronic focus. In the close proximity of the electronic focus, the lateral and longitudinal variability lower down to 22 µm and less. This study suggests that UDT allows for safer and more efficient procedures in a manner that is compatible with the current clinical workflow.

Keywords: Needle tip tracking, high resolution, optical sensing, optical hydrophone, nerve blocks, biopsy.

1. INTRODUCTION

Accurately and efficiently guiding a medical device, such as a needle or a catheter, to a target in the human body is of critical importance in a wide range of minimally invasive procedures, such as peripheral nerve blocks, central venous catheterizations, biopsies, and electrode insertions [1][2][3]. B-mode ultrasound is commonly used for guidance, but visualization of the device tip can be challenging [4]. Needle and catheter tips readily deviate from the imaging plane and they can have poor echogenicity at steep insertion angles. Optical techniques exist to perform spectroscopic differentiation of tissue structures on the needle path [5][6][7], but tracking of the needle tip position is necessary to ensure procedural safety[8][9][10][11].
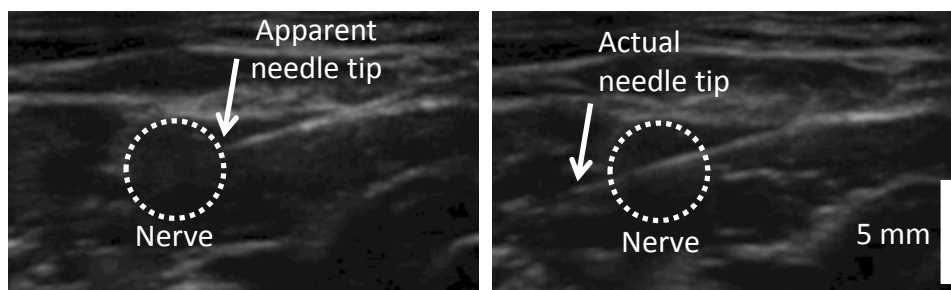

Figure 1: Challenges associated with ultrasound guidance; left: the partly visible needle (arrow), appears to have reached the vicinity of a nerve; right: repositioning the probe so that the needle tip is in plane reveals the true penetration depth of the needle that has already traversed the nerve. Nerve trauma is a complication that can lead to permanent loss of function. Needle tip tracking could allow these situations to be avoided.

During insertions, the needle tip can be indistinguishable from more proximal parts. As such, it can be significantly deeper in tissue than it appears with ultrasound imaging (Figure 1). Steep needle insertions, which are often required to

*jm.mari@ucl.ac.uk; phone +44 020 7679 0200; fax +44 (0)20 7679 0255

reach deep targets, result in small angles between the directions of the incident ultrasound beams and the needle shaft so that reflections from the needle surface may not be received, even with ultrasound image enhancement methods such as compound imaging or beam steering [12][13]. The uncertainties about the position of the needle tip elevate risks of severe complications including intraneural injection, intravascular injection, and pneumothorax [1][8][14][15]. Many methods have been proposed for improving the visibility of medical devices during ultrasound guided procedures: echogenic needles, which typically involve modifications to the surfaces of needles to increase the angular range of ultrasound backscattering, can be useful for steep insertion angles, but they are only relevant for needle parts that are in the imaging plane, so that they do not remove ambiguities about the position of the needle tip [16][17]. Methods such as shaft vibrations [18], electromagnetic tracking [19], Doppler imaging [20], ultrasound transmissions or reception [21] from the needle tip, and photoacoustic imaging [22] are also primarily relevant when the needle tip is in the imaging plane. Mechanical needle guides [23] and linear bearing devices [26], which can improve visibility by mechanically constraining a portion of the needle relative to the ultrasound imaging probe, require re-insertion of the needle during changes of trajectory, and they do not help if the needle bends out of the ultrasound imaging plane [23]. Three-dimensional (3D) ultrasound imaging can be used to provide visualisation of needles across a larger spatial volume than 2D imaging [13][16], but this imaging modality is currently expensive with bulky probes and inadequate resolution; as such, it is used infrequently in many clinical applications. Moreover, robust, real-time, automatic segmentation of needles from 3D images can be challenging.

In this study, we present a new tracking method that involves the detection of ultrasound with a sensor integrated into the medical device. Ultrasound pulses for localization were transmitted by the imaging probe and received by a fibre-optic hydrophone that was integrated into the medical device. Custom software was developed to generate ultrasound pulses for device localization, to receive signals from the hydrophone, and to acquire and display ultrasound images with the co-registered needle tip position.

2. METHODS

In order to implement ultrasonic device tracking (UDT), the ultrasound sensor must be sufficiently small to be inserted inside needles that are used in clinical practice without complicating their manipulation or occluding their lumens. Optical fibre hydrophone sensors, which were developed at the University College London, offer a combination of characteristics that are particularly well suited to UDT, as compared with conventional ultrasound sensors. They are broadband (50 MHz), they exhibit low directional sensitivity, and they can be thin (< 145 μm) [25]. When integrated into the lumen of an injection needle, the hydrophone (Precision Acoustics, Dorchester, UK) allowed for the detection of impinging ultrasound pulses from the imaging probe. It could be comfortably positioned into a 20-gauge spinal needle cannula, leaving most of the lumen free (Figure 2). With UDT, acquisition of hydrophone signals that were temporally synchronized with the B-mode ultrasound imaging transmissions [13] allowed for the position of the sensor and the corresponding position of the needle tip to be estimated.
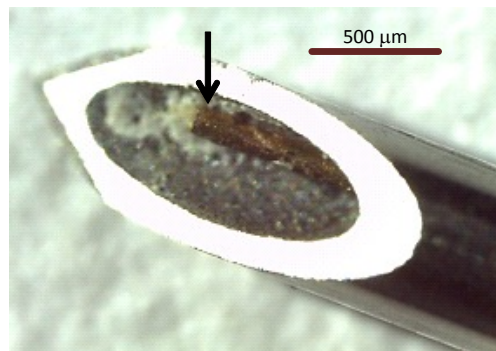

Figure 2. Photo of the tip of a 20 gauge needle with the distal end of the optical fibre hydrophone (arrow) positioned at the bevel to receive transmissions from the ultrasound imaging probe.

To detect ultrasound at the needle tip synchronously with the ultrasound B-mode transmissions, the setup described in Figure 3 was implemented. An ultrasound imaging system (MDP, Ultrasonix, Richmond, BC, Canada) equipped with a

L14-5/38 probe was programmed using the Labview programming language (National Instruments, Austin, TX, USA). This imaging system allows for imaging sequences to be defined using low-level libraries (Ultrasonix Texo.dll) and it provides line transmit synchronization signals with a BNC connector. The synchronization signals were used to trigger the acquisitions of optical hydrophone sensor signals with a National Instruments digital acquisition module (DAQ USB-5132). The second channel of the DAQ module sampled signals from the optical hydrophone sensor [25] at 100 MS/s; the resulting data was transferred to the ultrasound imaging system computer in the Labview environment where it was post processed and displayed in Labview using Matlab (Mathworks, Natick, Massachusetts, USA). The envelope of the RF data, which was transferred to Labview directly through memory copy, was displayed as the B-mode ultrasound image.
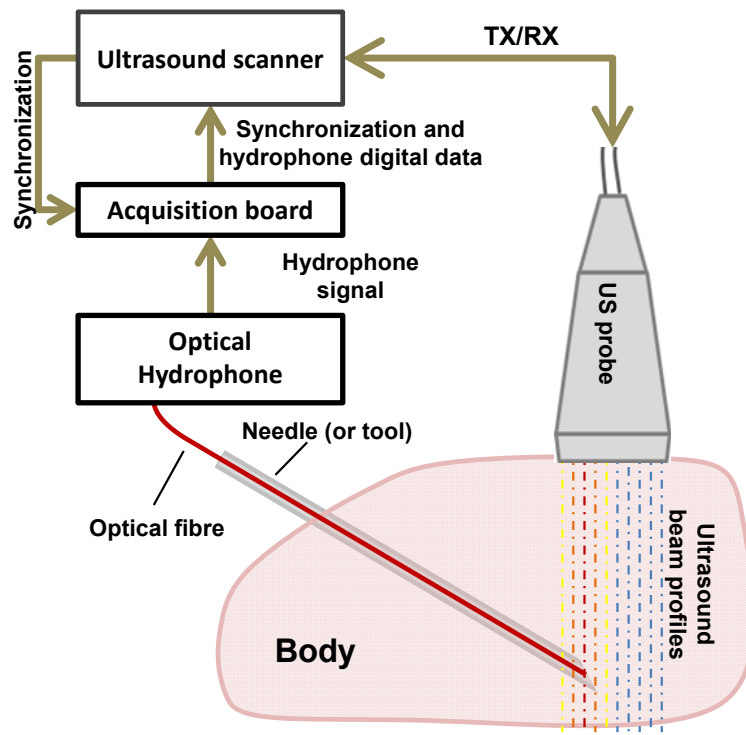

Figure 3: Principle of B-mode UDT collection: a line signal, generated by the ultrasound scanner each time a B-mode transmit occurs, is used to synchronized the acquisition of optical hydrophone signals, so that the estimated positions of the needle tip can be co-registered with the ultrasound images.

The transmit sequence of the Ultrasonix MDP ultrasound scanner was programmed using an in-house library to perform B-mode imaging with controlled transmit timings. Ultrasound transmissions from the imaging probe that were generated for B-mode imaging were the same ones used for UDT. There were 128 transmitted A-lines per image. As the ultrasound imaging probe had 128 elements, each element was the centre of the transmission aperture of a ultrasound A-line, so that the theoretical line spacing was that of the transducer element spacing: 300 μm. The maximum aperture size was 32 elements. The electronic focus was set to different values for the different experiments described below. The following parameters were used: transmit frequency 9.5 MHz, pulse length set to the shortest possible, data sampling rate at 40 MHz, transmission power was set to medium power (index 12 out of 15 on the Ultrasonix MDP scanner).

The position of the needle tip was estimated from the optical hydrophone sensor signal using two methods. With the first method, it was assumed that the ultrasound transmission that gave rise to the maximum signal amplitude was generated by a set of transducer elements that were directly above the needle tip. Accordingly, the lateral component of the position estimate was given by the lateral position of the central transducer element of this set. The depth component of the position estimate was obtained by multiplying the measured transmission time by the ultrasound speed in water. With the second method, the position was estimated as the centroid of the received hydrophone data. In the calculation of this centroid, the position values were weighted by the amplitude of the corresponding hydrophone data. With both methods, the estimated position of the needle tip was superimposed onto the ultrasound image with a red cross in real time.

Three experiments were performed to test UDT. In all of them, the bevel surface of the needle was turned upward to face the imaging probe and the needle tip was maintained in the imaging plane at an angle of approximately 45° (as measured relative to the surface).

In the first experiment, the system was tested visually to make a quick performance assessment. The needle was manually inserted into a nerve block phantom (Blue Phantom Regional Anesthesia Training Block Model, CAE Healthcare, Florida), with the practitioner trying to insert the needle towards a vessel structure without puncturing it.

In the second experiment, the needle was placed in a water bath, with the electronic focus of the ultrasound image set to 30 mm. Data from the optical hydrophone sensor was acquired for the needle tip positioned before, at, and after the electronic focus.

In the third experiment, the needle was placed in a water bath, with the electronic focus set to 40 mm. Using motorised positioning stages controlled by Labview (MTS50/M-Z8, Thorlabs Inc., Newton, NJ, USA), the needle was advanced so that its depth ranged from 20 to 60 mm in 10 steps. At each step, the needle was maintained in one position, and optical hydrophone sensor data was acquired 50 times to measure the position estimates.

3. RESULTS AND DISCUSSION

With needle insertions performed in the nerve block ultrasound phantom during the first experiment, good agreement was found between the position of the needle tip that was estimated with UDT and that which was observed on the B-mode ultrasound images.
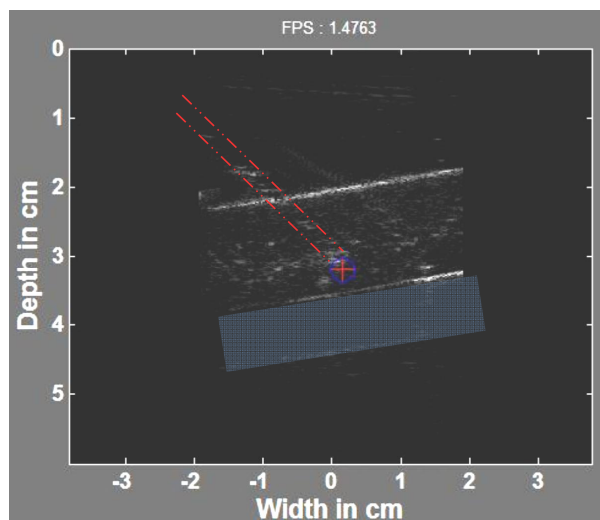

Figure 4: B-mode ultrasound image obtained during a needle insertion into a nerve block phantom. The position of the needle tip estimated with ultrasonic device tracking was displayed in real time with an overlaid red cross/blue circle. The needle shaft is apparent as a series of weak reflections (in-between the red dashed lines); a model blood vessel lies just beneath the estimated position (transparent rectangle). The red dashes and the transparent rectangle are provided to facilitate interpretation of this image and were not present in the real-time display.

An example of an ultrasound image with an overlaid position estimate is shown in Figure 4. The needle shaft was often poorly visible with ultrasound imaging, but UDT allowed for continuous position estimates to be provided. The operator was capable of getting the tip very close to the wall of the vessel mimicking structure without puncturing it.

The amplitudes of the optical hydrophone sensor signals, as measured in experiment 2, were typically maximal when the needle tip was directly below the transducer elements that generated the corresponding ultrasound transmissions. In general, the rate at which the amplitude changed with respect to the lateral position of the ultrasound transmissions was dependent on the depth of the needle tip relative to the electronic focus: the amplitude changed more slowly when the needle tip was away from the electronic focus (Figure 5).
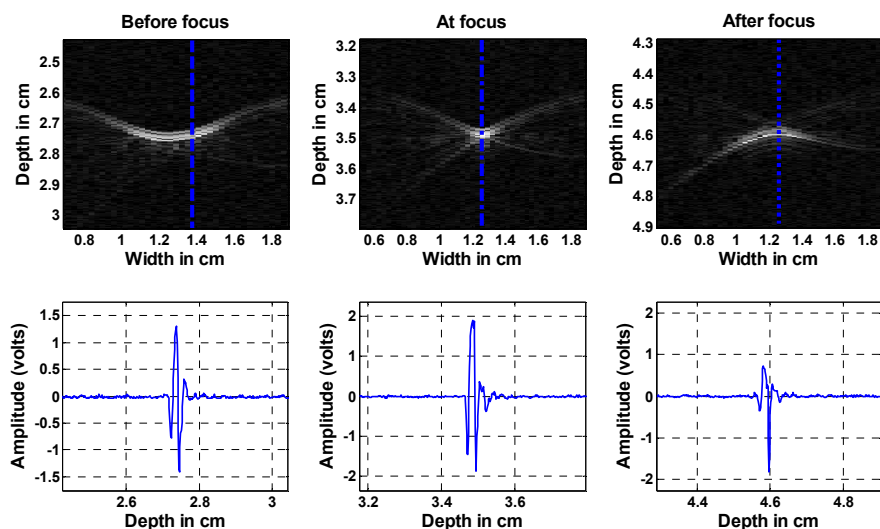
Figure 5: Optical hydrophone signals detected during transmissions from the ultrasound imaging probe. Top: signals acquired during consecutive ultrasound transmissions, concatenated and displayed according to their amplitudes in the same spatial coordinates as the B-mode ultrasound images. The depth of the needle tip varied from 2.75 mm (before the electronic focus), 3.5 mm (at the electronic focus), and 4.6 mm (after the electronic focus). Bottom: individual signals from which the maximum amplitude was obtained; their correspondence to the images is indicated with dashed blue lines.

The bottom plots of Figure 5 show the A-line profiles of the top images corresponding to the vertical line in the top row, where the maximum of signal was detected. In all three positions, the signal amplitude increases as the transmit centre elements get in line with the tip of the needle. The shape of the ultrasound pulse as sensed at the tip evolves progressively from the shallow regions to the deeper regions, the maximum amplitude being observed close to the electronic focus. While pre-electronic focus to electronic focus sensed pulse shapes remain similar, the post-electronic focus pulse shape is different.
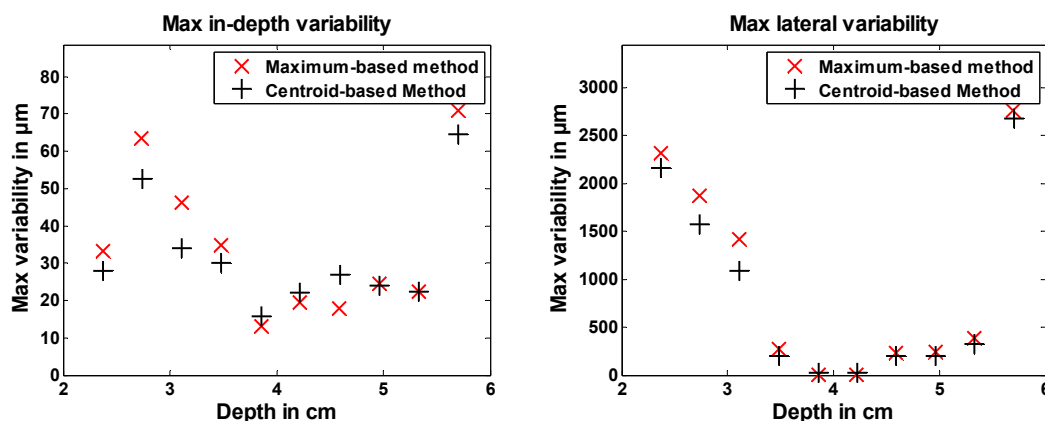

Figure 6: variability of the depth (left) and lateral (right) components of the position estimates, with the needle tip fixed in position at different depths and the electronic focus of the ultrasound images set to 40 mm. Estimates were obtained with the maximum-based and the centroid-based position estimation methods.

The results of experiment three are provided Figure 6, where the maximum distances between the average position of a repetition group and the farthest position found longitudinally (in-depth) and laterally (along the probe) are plotted. The distance to the electronic focus influences the maximum in-depth variability, and the maximum values close to the electronic focus are below 40 μm, but on the overall, the in-depth estimates are extremely precise and are all below 80 μm. But the lateral estimates can be much more variable, the positions closer to the ultrasound probe and the deeper one being above 1 mm, and close to 3 mm for the last one. This is due to the widening of the ultrasound beam before and

after the electronic focus, which, combined with noise, randomises the position of the maximum, and thus also of the position of the centroid. However in the vicinity of the electronic focus, the maximum variability remains below 500 μm.

The variability of the depth and lateral components of the position estimates was smallest for positions close to the focus. For the depth component of the position estimate, the variability was 13.24 μm / 15.9 μm at a depth of 38.5 mm, for maximum-/centroid-based estimates. The variability of the lateral component of the position estimate was 0 μm/22.2 μm at a depth of 38.5 mm for maximum-/centroid-based estimates. With the maximum-based estimation method, the lateral component of the position estimate was discretised according to the centre-to-centre separation of the ultrasound transducer elements (300 μm). This discretisation allowed for identically zero variability across multiple position estimates.

Beyond this proof-of-concept study, there are several ways in which the performance of ultrasonic device tracking could be improved. For instance, the estimates of the needle tip position could be used to dynamically adjust the electronic focus so that it is coincident with the needle tip and thereby to decrease variability. Additionally, the ultrasound transmissions used for B-mode imaging and those used for tracking could be distinct; the latter could be optimised using several approaches including single-element and coded pulse transmissions. While the current study was limited to tracking within the ultrasound imaging plane, new ultrasound imaging probes in which a subset of the ultrasound transmissions are performed outside the imaging plane will allow for tracking both inside and outside the imaging plane.

4. CONCLUSION

Even for experienced practitioners, accurate and efficient tracking of medical devices during ultrasound-guided procedures can be challenging. In this proof-of-concept study, a novel system for performing ultrasonic device tracking (UDT) of medical devices was presented. Ultrasound transmissions from the imaging probe were detected by an optical fibre hydrophone that was integrated into the cannula of an injection needle, and the hydrophone signals were processed to obtain estimates of the needle tip position. These position estimates were superimposed on B-mode ultrasound images in real-time. Two position estimation methods were considered. For both methods, the variability of the position estimates was shown to be smallest when the depth of the needle tip in the medium was coincident with the electronic focus of the ultrasound images. The maximum longitudinal variability remains below 80 μm for all distances of the needle tip to the electronic focus. The lateral variability remains below 500 μm in a 20 mm region around the electronic focus, but increases up to several mm away from the electronic focus. In the close proximity of the electronic focus, the variability achieved reduces down to 22 μm and below, and the method completely outperforms the other existing needle tracking techniques. Future research will attempt to further improve the quality of the overall tracking process by optimising the transmitted sequence, and maintain the optimum tracking capacities during the needle progression. UDT has strong potential to improve the efficiency and safety in a manner that is fully compatible with current clinical workflow.

REFERENCES

[1]   Marhofer, P., Chan, V. W. S., "Ultrasound-guided regional anesthesia. Current concepts and future trends". Anesth Analg., 1265-1269 (2007).
[2]   Brynolf, M., Sommer, M., Desjardins, A.E., van der Voort, M., Roggeveen, S., Bierhoff, W., Hendriks, B. H. W., Rathmell, J. P., Kessels, A. G. H., Söderman, M, Holmström, B., "Optical Detection of the Brachial Plexus for Peripheral Nerve Blocks: An in vivo Swine Study". Reg Anesth Pain Med., 36(4), 350–357 (2011).
[3]   Narouze, S. N, [Atlas of Ultrasound-Guided Procedures in Interventional Pain Management 1st ed]. Springer, New York, (2010).
[4]   Chin, K. J, Perlas, A, Chan, V. W. S., Brull, R. "Needle Visualization in Ultrasound-Guided Regional Anesthesia: Challenges and Solutions". Regional Anesthesia and Pain Medicine, 33(6):532-544 (2008).
[5]   Balthasar, A., Desjardins, A.E., van der Voort, M., Lucassen, G. W., Roggeveen, S., Wang, K., Bierhoff, W., Kessels, A. G. H., van Kleef, M., Sommer, M., "Optical Detection of Peripheral Nerves: An in vivo Human Study". Regional Anesthesia and Pain Medicine, 37 (3):277 (2012).
[6]   Desjardins, A. E, Hendriks, B. H. W., van der Voort, M., et al. "Epidural needle with embedded optical fibers for spectroscopic differentiation of tissue: ex vivo feasibility study". Biomed Opt Express., 2(6):1452-1461 (2011).

[7]   Desjardins, A. E., van der Voort, M., Roggeveen, S., et al. "Needle stylet with integrated optical fibers for spectroscopic contrast during peripheral nerve blocks" J Biomed Opt., 16(7):077004 (2011).

[8]   Chan, V. W. S, Perlas, A., McCartney, C. J. L., Brull, R., Xu, D. Q., Abbas, S. "Ultrasound guidance improves success rate of axillary brachial plexus block" Can J Anaesth., 176-182 (2007).

[9]   Hurdle, M. F., Weingarten, T. N., Crisostomo, R. A., Psimos, C., Smith, J., "Ultrasound-guided blockade of the lateral femoral cutaneous nerve: technical description and review of 10 cases" Arch Phys Med Rehabil., 1362-1364 (2007).

[10] Marhofer, P., Schrögendorfer, K., Wallner, T., Koinig, H., Mayer, N., Kapral, S. "Ultrasonographic guidance reduces the amount of local anesthetic for 3-in-1 blocks" Reg Anesth Pain Med., 584-588 (1998).

[11] Redborg, K. E, Sites, B. D., Chinn, C. D., et al. "Ultrasound improves the success rate of a sural nerve block at the ankle" Reg Anesth Pain Med. 24-28 (2009).

[12] Cobbold, R., [Foundations of Biomedical ultrasound], Oxford University Press (2007).

[13] Mari, J-M., Cachard, C., "Acquire real time RF digital ultrasound data from a commercial scanner". Technical Acoustics, (2007).

[14] Sites, B. D., Brull, R., Chan, V. W. S., et al. "Artifacts and pitfall errors associated with ultrasound-guided regional anesthesia". Reg Anesth Pain Med., S81-S92 (2010).

[15] Ting, C. K., Tsou, M. Y., Chen, P. T., et al. "A new technique to assist epidural needle placement: fiberoptic-guided insertion using two wavelengths" Anesthesiology., 1128-1135 (2010).

[16] Mari, J-M., Cachard C., "Ultrasonic scanning of straight micro tools in soft biological tissues: methodology and implementation" Ultrasonics, 51(5):632-63, (2011).

[17] Uhercik, M., Barva, M., Kybic, J., Mari, J-M., Duhamel, J-R., Hlaváč, V., Cachard, C., "Parallel integral projection transform for electrode localization in 3D ultrasound images" IEEE Trans. UFFC, 55(7): 1559-1569 (2008).

[18] Harmat, A, Rohling, R. N., Salcudean, S. E., "Needle tip localization using stylet vibration" Ultrasound in Medicine & Biology, 32(9) 1339-1348 (2006).

[19] Krücker, J., Xu, S., Glossop, N., Viswanathan, A., Borgert, J., Schulz H., Wood, B. J., "Electromagnetic Tracking for Thermal Ablation and Biopsy Guidance: Clinical Evaluation of Spatial Accuracy" J Vasc Interv Radiol., 1141-50 (2007).

[20] Tsung, J. W, Blaivas, M, Stone, M. B., "Feasibility of point-of-care colour Doppler ultrasound confirmation of intraosseous needle placement during resuscitation" Resuscitation, 80(6):665-668 (2009).

[21] Mung, J., Vignon, F, Jain, A. "A non-disruptive technology for robust 3D tool tracking for ultrasound-guided interventions" Med Image Comput Comput Assist Interv., 153-60 (2011).

[22] Piras, D., Grijsen, C., Schütte, P., Steenbergen, W., Manohar, S., "Photoacoustic needle: minimally invasive guidance to biopsy" Journal of Biomedical Optics, 18(7), 070502 (2013).

[23] Weller, R. S, "Misaligned mechanical ultrasound transducer contributes to carotid puncture" Seminars in Anesthesia, Perioperative Medicine and Pain, 193-196 (2007).

[24] van Geffen, G. J., Mulder, J., Gielen, M., van Egmond, J., Scheffer, GJ, Bruhn, J., "A needle guidance device compared to free hand technique in an ultrasound-guided interventional task using a phantom" Anaesthesia., 986-90 (2008).

[25] Morris, P., Hurrell, A., Shaw, A., Zhang, E., Beard, P. C., "A Fabry–Pérot fiber-optic ultrasonic hydrophone for the simultaneous measurement of temperature and acoustic pressure" J. Acoust. Soc. Am., 3611-3622, (2009).

[26] Stuber, V., Suero, E. M., Hufner, T., Wiewiorski, M., Krettek, C., Citak, M., "Linear bearing device as a solution for optical navigation of fine needle procedures" Technology and Health Care, 18: 267–273 (2010).